Mechanics of Advanced Composite Structures 2 (2015) 127-134

Semnan University

Mechanics of Advanced Composite Structures

journal homepage: http://MACS.journals.semnan.ac.ir

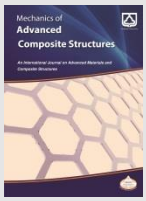

Damage Energy Evaluation in [55/-55]$_9$ Composite Pipes using Acoustic Emission Method

H.R. Mahdavi[a], G.H. Rahimi[a*], A. Farrokhabadi[a], H. Saadatmand[b]

[a]*Faculty of MechanicalEengineering, Tarbiat Modares University, Tehran, Iran*
[b]*Department of Engineering Design, National Iranian Gas Company, Boushehr, Iran*

PAPER INFO

Paper history:
Received 7 November 2015
Received in revised form 3 December 2015
Accepted 4 December 2015

Keywords:
GRE composite pipe
Longitudinal strength
Hoop strength
Acoustic emission
Failure mechanisms

ABSTRACT

In this study, the longitudinal and hoop tensile strengths of an industrial ±55° Glass Reinforced Epoxy (GRE) pipe with eighteen layers as well as the associated failure mechanisms are determined. To obtain the longitudinal and hoop tensile strengths values, three specimens are cut from the studied GRE pipe in each direction. A comparison is done between both the strength values, and the fracture pattern of the specimens is studied. Determining the different failure mechanisms which are created during both of the tests, the acoustic emission technique is used. The acoustic emission energy as an important damage parameter in determining the different failure mechanisms of the specimens is depicted for both of the tests and is related to the obtained results from the stress-time curve. A high magnification camera is used to verify the failure mechanisms characterized by the acoustic emission method.

1. Introduction

Nowadays, filament-wound GRE pipes are used in a number of industries such as aerospace, oil and gass etc. due to the good corrosion resistance and high strength to weight ratio. Thus, determination of the longitudinal and hoop tensile strength and characterization of the failure mechanisms of these pipes are important issues.

A number of researches have been done in the field of longitudinal and hoop tensile strenghth of the composite pipes up to now. Choen [1] investigated the influence of the filament winding parameters on the composite vessel quality and strength. Choen et al. [2] explored the fiber volume fraction effect on the composite pressure vessel strength. Xia et al. [3] analyzed the multi-layered filament-wound composite pipes under the internal pressure. They obtained exact solutions for distribution of the hoop and axial stresses through the non-dimensional radius distance. Hwang et al. [4] examined the size effect on the fiber strength of the composite pressure vessels using analytical and experimental approaches. Baranger et al. [5] propose a computational strategy for the analysis of damage that is caused by manufacturing defects in the composite pipes. Melo et al. [6] investigated the mechanical behavior of Glass Reinforced Polymer (GRP) pipes by adding the quartz sand filler experimentally throughout the short-time hydraulic failure pressure tests. Rafiee [7] calculated the hoop tensile strength of the GRP pipes with different geometry, number of layers, and filament-wound angle using experimental, theoretical, and numerical methods.

The acoustic emission is often defined as ‘‘the release of transient elastic waves produced by a rapid

*Corresponding author, Tel: +98-21-82883356; Fax: +98-21-88006544

E-mail address: rahimi_gh@modares.ac.ir

redistribution of stress in a material [8]. Curtis [9] concludes that the energy in the acoustic waveform is proportional to the energy of the associated deformation. As a result, the larger cracks emit higher energy than the micro-cracks. Groot et al. [10] investigated the different failure mechanisms of the carbon/epoxy composites using the acoustic emission. Yu et al. [11] studied the failure detection of the composite materials using the acoustic emission. Bourchak et al. [12] tested the carbon fiber reinforced plastic composite laminates under the static and fatigue loading. They use the acoustic emission technique for failure mechanisms detection and conclude the acoustic emission energy is an important parameter in evaluating the failure mechanisms of the specimens. Bussiba et al. [13] explored the damage evolution and fracture events sequence in uniform and notched composite specimens under the quasi-static loading in uniaxial and bending modes using the acoustic emission. De Rosa et al. [14] presented a literature review of AE applications in the studies on the natural fiber composites. Liu et al. [15] studied the failure mechanisms of the carbon fiber/epoxy composite laminates with different layup patterns and central hole size arrangements using the acoustic emission technique. Aggelis et al. [16] studied the characterization of the damage state in cross ply laminates using the acoustic emission and ultrasonics. Zarif Karimi et al. [17] monitored the residual tensile strength of the drilled composite laminates using acoustic emission. Belalpour dastjerdi et al. [18] investigated the initiation and growth of the delamination in the composite materials using the acoustic emission. Saeedifar et al. [19] classified the damage mechanisms during the delamination growth in the sandwich composites using acoustic emission. Ben Ammar et al. [20] used the mechanical behavior and acoustic emission method for detecting the damage in the sandwich composite materials. Navid Zarif Karimi et al. [21] analysed the damage mechanisms of the composite materials in the drilling process using acoustic emission. However, according to the knowledge of the authors, no serious study has been done in the field of failure mechanisms detection of the composite pipes by analyzing the acoustic emission energy values. The main objective of the present study is to determine the longitudinal and hoop tensile strengths of an industrial filament-wound GRE pipe as well as the associated failure mechanisms. To characterize the failure mechanisms of the specimens, the acoustic emission technique is used. The acoustic emission energy in the longitudinal and hoop specimens is recorded during the tests in terms of the time and is compared with the stress-time curve. The relevant failure mechanisms created in the specimens are characterized using the high magnification camera, too.

2. Experimental Procedure

An industrial $(\pm 55^{\circ})_9$ filament-wound GRE pipe with eighteen antisymmetric layers is used for studying. The inner diameter and total thickness of the studied GRE pipe are 209 mm and 6.3 mm, respectively. The ASTM D-3039 standard is used for determination of the longitudinal tensile strength of the specimens [22]. According to this standard, three specimens are cut in the longitudinal direction from the studied GRE pipe. The width and thickness of the specimens are 25 mm and 6.3 mm, respectively. Based on the standard, the following equation is used to calculate the longitudinal strength [22]:

$$S_L = F_f/(wt) \quad (1)$$

In the above equation, S_L *(MPa)*, F_f *(N)*, W *(mm)* and t *(mm)* are the longitudinal strength, failure load, width, and thickness of the specimens, respectively. The ASTM D-2290 standard is used for determination of the apparent hoop tensile strength of the specimens [23]. This standard proposes a method for determination of the apparent hoop tensile strength of the composite pipes. The reason for using an apparent hoop tensile strength rather than a true hoop tensile strength is the imposed bending moment during the tests [23].

Fig. 1 shows the imposed bending moment in the hoop specimen. It is necessary to mention that the design of the fixtures for appling the load is in a manner that the bending moment is reduced [7, 23]. Based on the ASTM D-2290, three ring specimens are cut from the mentioned GRE pipe using the milling machine with overall width of 24 mm [23]. In addition, two reduced areas are created at the angle of 180° from each other with width of 14 mm [23]. According to this standard, the hoop strength of the specimens is calculated using the following equation [23]:

$$S_H = F_f/(2wt) \quad (2)$$

In the above equation, S_H *(MPa)*, F_f *(N)*, W *(mm)* and t *(mm)* are hoop strength, failure load, width, and thickness of the specimens, respectively. Fig. 2 shows the cut in the longitudinal and hoop specimens. The fiber volume fraction is determined in accordance with the ASTM D-2584 standard using the burn-off test [24]. For this purpose, an element of the GRE pipe is cut with the specific weight and is placed in an oven. The element is heated up to 600°C until all its resin content is burnt. After the test, the fiber volume fraction is found to be 49.09%. The mechanical properties of the glass fiber and resin are stated in Table 1 [25].

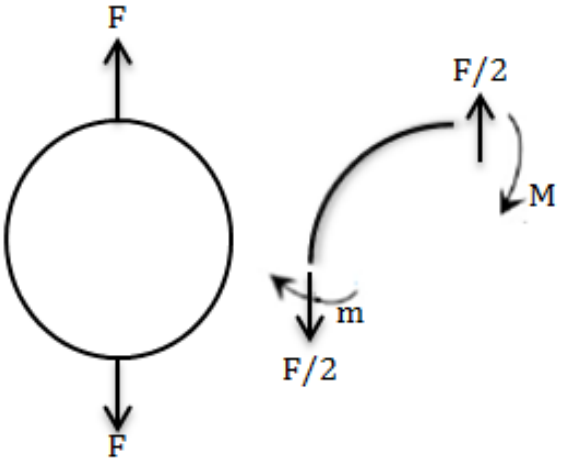

Figure 1. The induced moment in the hoop specimen

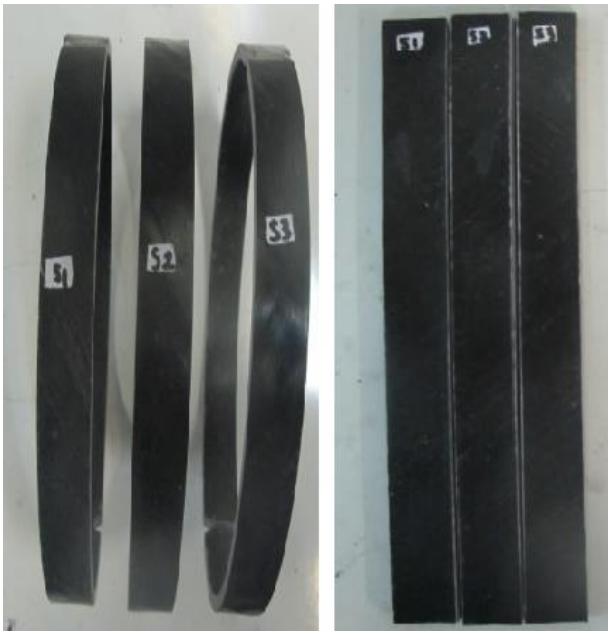

Figure 2. The hoop specimens (left picture) and longitudinal specimens (right picture)

Table 1. The mechanical properties of the glass fiber and resin [25]

Material	E (GPa)	σ_{ut} (MPa)	ρ (g/cm^3)	ε_{max}
E-Glass	72.3	3445	2.58	4.8
Epoxy	2.75	69	1.16	3

The tensile tests are conducted in a 30 KN Shijin wdw.300e universal testing machine with the hydraulic clamping fixtures. The displacement control mode is accepted for both of the tests. The rate of loading is set at 2 and 3 mm/min in the longitudinal and hoop specimens, respectively [22, 23]. In addition, according to the shape of the hoop specimens and limitations of the testing machine, a specific fixture is designed which is called split disk.

The acoustic emission signals are recorded with Vallen AMSY-6 system. Two wideband sensors are attached to the longitudinal and hoop specimens using REF 1171-002 ultrasonic gel as coupling. The sensors have an operating frequency range of 20-450 kHz with a peak frequency of 275 kHz. The signals are amplified using the AEP4 preamplifiers with a gain of 40 dB. The ambient noise is filtered using a threshold of 38.1 dB.

In general, the acoustic emission energy is computed as the integral of square of the signal amplitude measured in volts ($V_i(t)$) over the signal duration (t_1-t_0) measured in second according to the following equation [26, 27]:

$$E_i = \int_{t_0}^{t_1} V_i^2(t)dt \quad (3)$$

In the above equation, i, t_0, and t_1 have the following meanings:

i= the recorded voltage transient $V(t)$ of a channel

t_0= the starting time of the voltage transient record

t_1= the ending time of the voltage transient record

It is necessary to mention the channel word is representative of the single acoustic emission sensor and the related measurement and processing instrumentation [28]. Fig. 3 shows the necessary equipment for the acoustic emission test. The attached sensors to one of the test specimens and the split disk test fixture, as well as the universal testing machine are shown in Fig. 4 (a,b).

3. Results and Discussion

In this section, at first, the obtained results are presented for the longitudinal specimens, and then the results of the hoop specimens are stated. In both specimens, the obtained strength of three tests is proposed, and the corresponding average value and the standard deviation are reported. The AE data results are expressed for one of the three test specimens. Also, some of the relevant failure mechanisms characterized in the longitudinal and hoop specimens are presented.

3.1. The longitudinal specimens

The obtained results of the three tests for the longitudinal strength are depicted in Fig. 5. According to the figure, the obtained strength values for the specimens are 76.73, 74.04, and 74.18 MPa, respectively.

According to the strength values, the average and standard deviation are calculated to be 74.94 MPa and 1.74, respectively. Fig. 6 shows the stress-strain curves for the longitudinal specimens. Based on the figure, a relatively bilinear behavior is seen in the specimens.

Fig. 7 shows the obtained stress-time behavior and the recorded acoustic emission energy during the test for the specimen with the strength of 74.04 MPa. For a better interpretation of the results, the recorded acoustic emission energy axis is scaled.

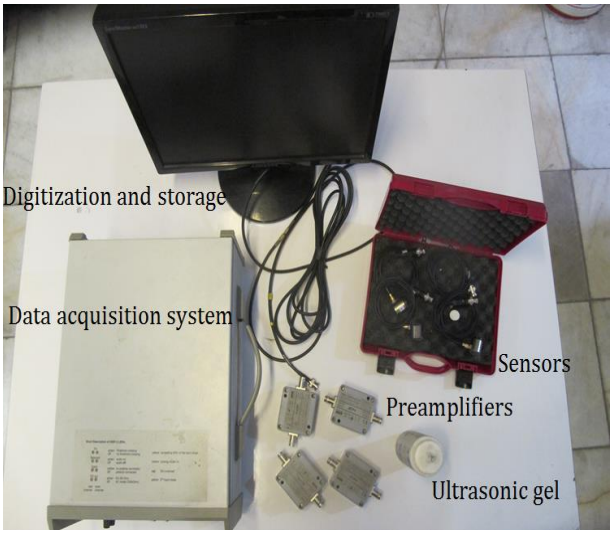

Figure 3. The required equipment for capturing the acoustic emission signals

(a)

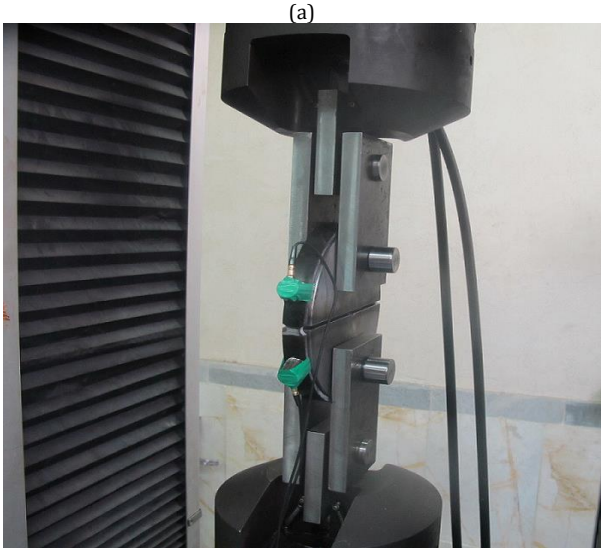

(b)

Figure 4. The longitudinal and hoop specimens: (a) Longitudinal specimen, (b) Hoop specimen

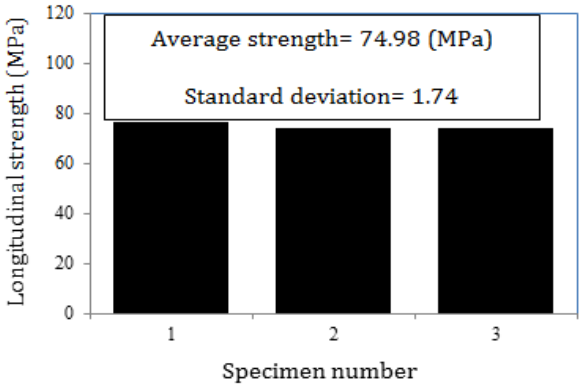

Figure 5. The strength values for the longitudinal specimens

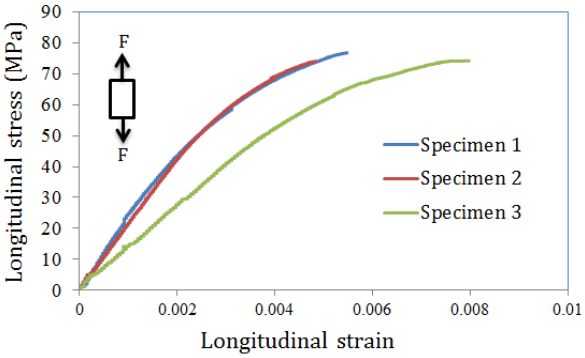

Figure 6. The stress-strain curves for the longitudinal specimens

According to the figure, the damage evolution can be classified into three stages: at the first stage (0-159 s), no noticeable damage is detected, and the significant damage is commenced at the end of this stage, i.e. in 159 s. At this moment, the applied stress to the specimen is found to be 32.23 MPa, i.e. 44% ultimate strength of the specimen, and the induced strain in the specimen is equal to 0.00152. Also, the energy is about $2.16e^{7}$ attojoule (1 attojoule = $1e^{-18}$ joule). This stage of damage can be considered as the damage initiation stage, in which some microscopic cracks are created in the matrix and fiber and matrix interface (matrix microcracking). At the second damage stage (159-255 s), a steady state in the energy is observed until 255 s. In 255 s, a significant increase is observed in the energy level representing the formation of a new damage level in the specimen prior to the final failure. The corresponding induced stress and strain in the specimen are estimated to be 65.76 MPa, i.e. 0.89% ultimate strength of the specimen and 0.00368, respectively. It is necessary to note that the energy reaches about $2.15e^{7}$ attojoule, i.e. about 1.16 times energy level at the end of the first damage stage. This stage can be considered as the damage propagation stage, in which the created cracks in matrix and interface of fiber and matrix are joined together. Consequently, the density of the cracks reaches to a saturation state, and the conditions are provided for creating the

delamination damage mode (delamination). At the third or final damage stage (255-300 s), the severity of damage levels increases significantly, and finally, the fracture of the specimen happens corresponding to the maximum applied load releasing the huge amount of energy i.e. $3.66e^{9}$ attojoule (fiber pull-out and breakage) (it isn't observed in the graph due to change of the scale of the curve). This fact shows the crack density role in the released acoustic emission energy level [9].

Fig. 8 shows the surface image of the specimen after the final fracture. According to the figure, the final fracture of the specimen occurs at an angle of 55° with respect to the longitudinal axis, i.e. parallel to the plies at an angle of 55° and perpendicular to the -55° reinforced plies.

In Fig. 9, the captured images from some relevant failure modes such as delamination, fiber pull-out and fiber breakage are shown using a high magnification camera.

3.2. The hoop specimens

After testing three hoop specimens, the values of strength are found to be 261.48, 267.24, and 250.48MPa, respectively (average value=259.79 and standard deviation=8.42) which are shown in Fig. 10.

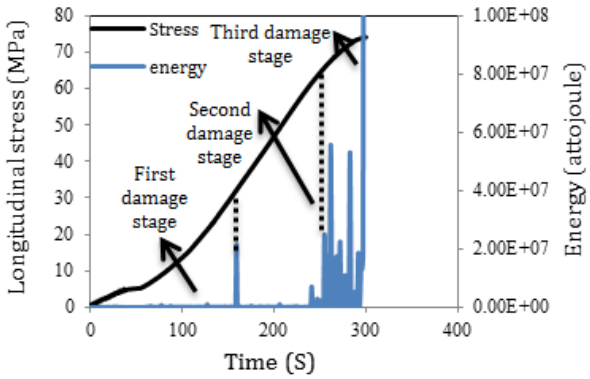

Figure 7. The obtained stress-time behavior and the recorded acoustic emission energy for the specimen with strength of 74.04 (MPa)

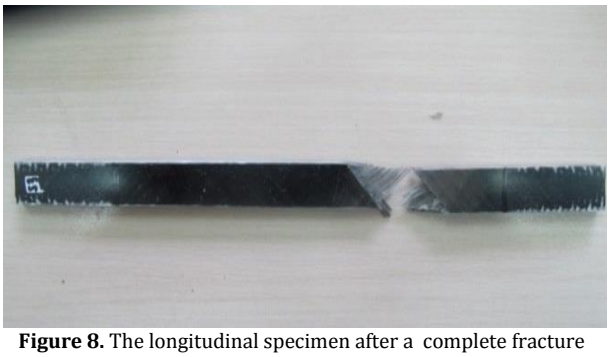

Figure 8. The longitudinal specimen after a complete fracture

Fig. 11 shows the load-deformation curves for the hoop specimens. According to the figure, a compeletely brittle behavior is seen in the specimens, and by releasing the load to the maximum value, the specimens are suddenly fractured.

In Fig. 12, the stress and energy versus the time are depicted for the specimen with the strength of 261.48 MPa. The energy axis is scaled such the longitudinal specimen. Similar to the longitudinal specimen, three damage stages can be considered. The start of a significant damage is at the end of the first damage evolution time, i.e. 75 s. At this time, the applied stress to the specimen is found to be 153.2 MPa, i.e. 58% ultimate strength of the specimen. The energy released from the specimen reaches $1.24e^{7}$ attojoule (matrix microcracking). At 126 s, a new severe damage level is created in the specimen. The applied stress in the specimen and the released energy from it reach to 246.53 MPa corresponding to 94% ultimate strength of the specimen and $6.14e^{7}$, respectively [9] (delamination). After this time, the creation of the new damage levels is continued in the specimen, and finally the specimen is fractured (fiber pull-out and breakage).

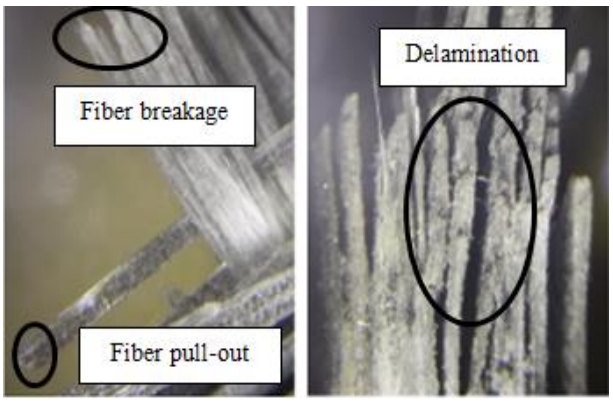

Figure 9. The captured images from the fracture mechanisms of the longitudinal specimens using a high magnification camera

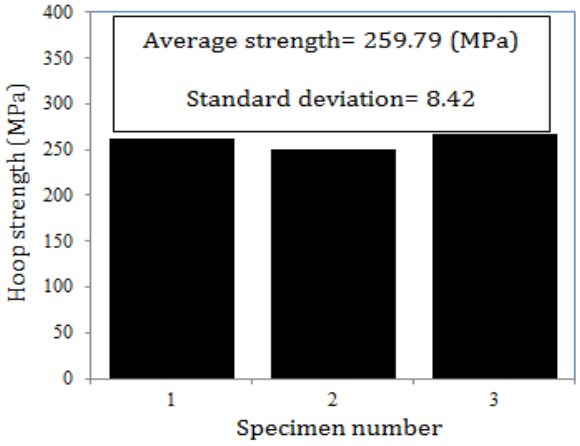

Figure 10. The strength values for the hoop specimens

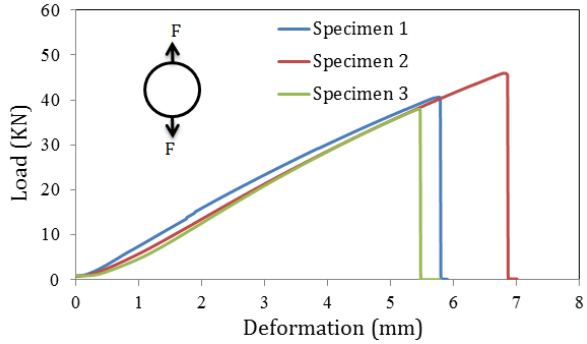

Figure 11. The load-displacement curves for the hoop specimens

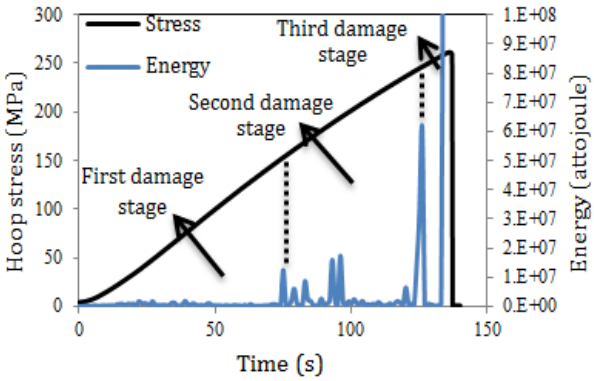

Figure 12. The stress and energy versus the time for specimen with strength of 261.48 (MPa)

Fig. 13 shows the surface image of the specimen after the final fracture. Based on the figure, the fracture behavior of the specimen with respect to the fracture angle is similar to the longitudinal specimen. The captured images from the relevant failure mechanisms are shown in Fig. 14 (a,b).

Based on Figs. 13 and 14, it can be concluded that the fracture of the specimens started with matrix cracking and fiber-matrix interface deboned in +55° reinforced plies continued by delamination, and it is completed with a fiber pull-out and breakage.

Figure 13. The hoop specimen after the complete fracture

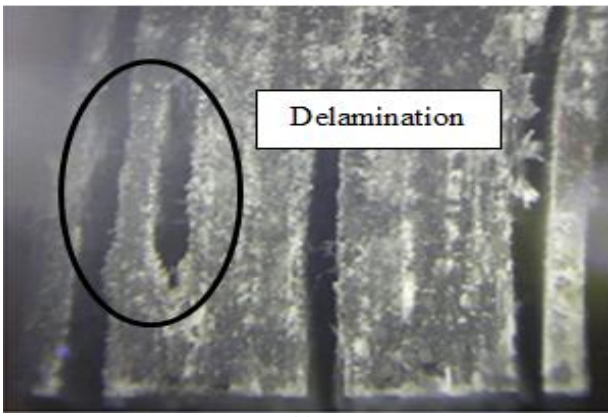

(a)

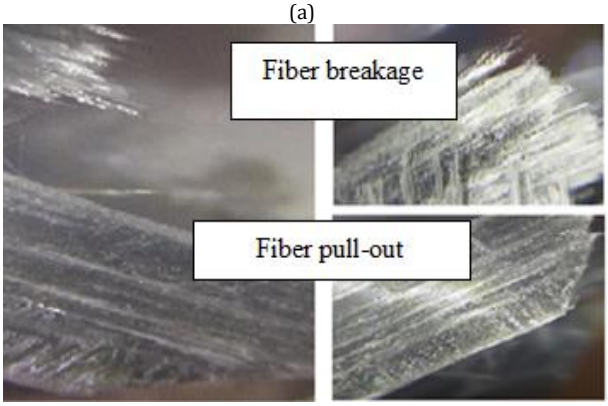

(b)

Figure 14. The captured images from the fracture mechanisms of the hoop specimens using a high magnification camera: (a) the delamination, (b) the fiber pull-out and fracture

4. Conclusion

In this study, the longitudinal and hoop tensile strengths values of an industrial ±55° GRE pipe with eighteen layers are determined. The results show the strength of the hoop specimens is about 3.5 times more than the longitudinal ones. A brittle behavior can be seen in the hoop specimens, while a relatively bilinear behavior is seen in the longitudinal specimens. The acoustic emission energy as an important damage parameter is recorded in both of the longitudinal and hoop specimens and is compared with the stree-time curve. According to the obtained acoustic emission energy values, the failure process is classified into three stages: damage initiation, damage propagation, and final fracture. The results show that in both of the longitudinal and hoop specimens the significante damge is started in a stress near to 50% ultimate strength and is propagated in a stress corresponding to the 90% ultimate strength of the specimens. The level of energy in each stage of failure can be acceptably associated with the density of the created cracks. Accordingly, the different failure mechanisms such as the matrix microcracking, delamination, fiber pull-out, and fiber breakage are characterized. Also, both of the specimens have a similar behavior from the damage initiation, damage propagation, and final fracture

points of view. The characterized failure mechanisms observed using a high magnification camera are acceptably in accordance with the obtained results from the acoustic emission energy analysis, too.

Acknowledgements

This study is supported by the research found of National Iranian Gas Company at Boushehr (NIGC - Boushehr).

References

[1] Cohen D. Influence of filament winding parameters on composite vessel quality and strength. *Compos Part A* 1997; 28: 1035-1047.

[2] Cohen D, Mantell SC, Zhao L. The effect of fiber volume fraction on filament wound composite pressure vessel strength. *Compos Part B* 2001; 32: 413-429.

[3] Xia M, Takayanagi H, Kemmochi K. Analysis of multi-layered filament-wound composite pipes under internal pressure. *Compos Struct* 2001; 53: 483-491.

[4] Hwang TK, Hong CS, Kim CG. Size effect on the fiber strength of composite pressure vessels. *Compos Struct* 2003; 59: 489-498.

[5] Baranger E, Allix O, Blanchard L. A computational strategy for the analysis of damage in composite pipes. *Compos Sci Technol* 2009; 69: 88-92.

[6] Melo JDZ, Neto FL, de Araujo Barros G, de Almeida Mesquita FN. Mechanical behavior of GRP pressure pipes with addition of quartz sand filler. *J Compos Mater* 2010; 45(6): 717-726.

[7] Rafiee R. Experimental and theoretical investigations on the failure of filament wound GRP pipes. *Compos Part B* 2013; 45: 257-267.

[8] Prosser WH. **Acoustic emission, In Shull PJ (Ed) Nondestructive Evaluation, theory, techniques and applications**. Taylor and Francis, 2002.

[9] Curtis GJ. Acoustic emission energy relates to bond strength. *Nondestr Test Eval* 1975: 249-257.

[10] Groot PJ, Wijnen PAM, Janssen RBF. Real-time frequency determination of acoustic emission for different fracture mechanisms in carbon/epoxy composites. *Compos Sci Technol* 1995; 55: 405-412.

[11] Yu YH, Choi JH, Kweon JH, Kim DH. A study on the failure detection of composite materials using an acoustic emission. *Compos Struct* 2006; 75: 163-169.

[12] Bourchak M, Farrow IR, Bond IP, Rowland CW, Menan F. Acoustic emission energy as a fatigue damage parameter for CFRP composites. *Int J Fatigue* 2007; 29: 457-470.

[13] Bussiba A, Kupiec M, Ifergane S, Piat R, Bohlke T. Damage evolution and fracture events sequence in various composites by acoustic emission technique. *Compos Sci Technol* 2008; 68: 1144-1155.

[14] De Rosa LM, Santulli C, Sarasini F. Acoustic emission for monitoring the mechanical behavior of natural fibre composites: A literature review. *Compos Part A* 2010; 40: 1456-1469.

[15] Liu PF, Chu JK, Liu YL, Zheng JY. A study on the failure mechanisms of carbon fiber/epoxy composite laminates using acoustic emission. *Mater Des* 2012; 37: 228-235.

[16] Aggelis DG, Barkoula NM, Matikas TE, Paipetis AS. Acoustic structural health monitoring of composite materials: Damage identification and evaluation in cross ply laminates using acoustic emission and ultrasonics. *Compos Sci Technol* 2012; 72: 1127-1133.

[17] Zarif Karimi N, Heidary H, Ahmadi M, Rahimi A. M. Farajpur. Monitoring of residual tensile strength in drilled composite laminates by acoustic emission. *Modares Mech Eng* 2013; 13(15): 169-183 (in Persian).

[18] Belalpour dastjerdi P, Fotouhi M, Fotouhi S, Ahmadi M. Acoustic emission based study to investigate the initiation and growth of delamination in composite materials. *Modares Mech Eng* 2014; 14(3): 78-84 (in Persian).

[19] Saeedifar M, Fotouhi M, Mohammadi R, Hajikhani M, Ahmadinajafabadi M. Classification of damage mechanisms during delamination growth in sandwich composites byacoustic emission. *Modares Mech Eng* 2014; 14(6): 144-152 (in Persian).

[20] Ben Ammar I, Karra C, El Mahi A, El Guerjouma R, Haddar M. Mechanical behavior and acoustic emission technique for detecting damage in sandwich structures. *Appl Acoust* 2014; 86: 106-117.

[21] Zarif Karimi N, Minak G, Kianfar P. Analysis of damage mechanisms in drilling of composite materials by acoustic emission. *Compos Struct* 2015; 131: 107-114.

[22] **Standard Test Method for tensile properties of polymer matrix composite materials**. Annual Book of ASTM Standard. D 3039-00; 2000.

[23] **Standard Test Method for Apparent Hoop Tensile Strength of Plastic or Reinforced Plastic Pipe by Split Disk Method**. Annual Book of ASTM Standard. D 2290-04; 2004.

[24] **Standard Test Method for Ignition Loss of Cured Reinforced Resins**. Annual Book of ASTM Standard. D 2584-02; 2002.
[25] Behroozi H. National Iranian Gas Company (NIGC), Boushehr, Iran, 2015.
[26] **Non-destructive testing -Acoustic emission- Equipment characterization- Part 2: Verification of operating characteristic.** BSI Standards Publication. BS EN 13477-2; 2010.
[27] Vidya Sagar R. An experimental Study on Acoustic Emission Energy and Fracture Energy of Concrete. *Proc National Semin Exhibition on Non-Destr Eval* 2009: 10-12.
[28] **Non-destructive testing- Terminology- Part 9: Terms used in acoustic emission testing.** Brithish Standard. BS EN 1330-9; 2009.